AD-A258 431

(2)

ARMY RESEARCH LABORATORY

A HIGHER ORDER EXPONENTIAL FUNCTION FOR FITTING NONLINEAR CURVES

Henry Rachele
Lisa Manguso
U.S. Army Research Laboratory

Neal H. Kilmer
Physical Science Laboratory
New Mexico State University
Las Cruces, New Mexico 88003

ARL-MR-24 *December 1992*

Approved for public release; distribution unlimited.

NOTICES

Disclaimers

The findings in this report are not to be construed as an official Department of the Army position, unless so designated by other authorized documents.

The citation of trade names and names of manufacturers in this report is not to be construed as official Government indorsement or approval of commercial products or services referenced herein.

Destruction Notice

When this document is no longer needed, destroy it by any method that will prevent disclosure of its contents or reconstruction of the document.

REPORT DOCUMENTATION PAGE

Form Approved
OMB No 0704-0188

1. AGENCY USE ONLY *(Leave blank)*

2. REPORT DATE
December 1992

3. REPORT TYPE AND DATES COVERED
Final

4. TITLE AND SUBTITLE
A HIGHER ORDER EXPONENTIAL FUNCTION FOR FITTING NONLINEAR CURVES

5. FUNDING NUMBERS
61102/53A (6.1)

6. AUTHOR(S)
Henry Rachele and Lisa Manguso
Neal H. Kilmer*

7. PERFORMING ORGANIZATION NAME(S) AND ADDRESS(ES)
U.S. Army Research Laboratory
Battlefield Environment Directorate
White Sands Missile Range, NM 88002-5501

8. PERFORMING ORGANIZATION REPORT NUMBER
ARL-MR-24

9. SPONSORING/MONITORING AGENCY NAME(S) AND ADDRESS(ES)
U.S. Army Research Laboratory
2800 Powder Mill Road
Adelphi, MD 20783-1145

10. SPONSORING/MONITORING AGENCY REPORT NUMBER

11. SUPPLEMENTARY NOTES
*Physical Science Laboratory
New Mexico State University
Las Cruces, New Mexico 88003

12a. DISTRIBUTION AVAILABILITY STATEMENT
Approved for public release; distribution unlimited.

12b. DISTRIBUTION CODE

13. ABSTRACT *(Maximum 200 words)*
Numerous mathematical methods have evolved over the years for fitting curves that exhibit nonlinear character. In this technical memorandum, the authors present a continuous function, the Rachele/Kilmer (R/K) optical profile function, that was originally configured by R/K to fit model simulated vertical profiles of extinction and backscatter coefficients in very low stratus clouds and subcloud regions. The R/K function fits most of the nonlinear optical profiles so well that the authors were encouraged to investigate its potential for fitting nonlinear curves that were produced by other physical/mathematical models. Results are presented that demonstrate the versatility and power of the R/K function when fitting simulated data from three different models.

14. SUBJECT TERMS
Nonlinear curve fitting, extinction, backscatter

15. NUMBER OF PAGES
13

16. PRICE CODE

17. SECURITY CLASSIFICATION OF REPORT	18. SECURITY CLASSIFICATION OF THIS PAGE	19. SECURITY CLASSIFICATION OF ABSTRACT	20. LIMITATION OF ABSTRACT
Unclassified	Unclassified	Unclassified	SAR

NSN 7540-01-280-5500

Standard Form 298 (Rev 2-89)
Prescribed by ANSI Std Z39-18
298-102

CONTENTS

LIST OF FIGURES

1. INTRODUCTION

The purpose of this technical memorandum is to present the R/K optical profile function and several graphical comparisons that illustrate the power and versatility of the function to fit nonlinear curves. Here, we did not review or present any of the multitude of mathematical curve fitting methods that are presented in numerous texts and papers. Instead, we focussed on the R/K functional form that we found to fit most of the vertical profiles of extinction and backscatter coefficients that were simulated by our theoretically based microphysics model (Rachele and Kilmer, 1992). The R/K function did not evolve without considerable effort. We had tried fitting extinction (σ_e) and backscatter (β) profile curves with other standard and nonstandard functional forms and approaches, but we were not consistently successful. One of these approaches involved calculating $\sigma_e(z + h)$ versus $\sigma_e(z)$ data, where z is height above ground level and h is a constant height increment, as proposed by Duncan et al. (1980). Those $\sigma_e(z + h)$ versus $\sigma_e(z)$ data were transformed (by rotation and/or translation of axes), and fitting functions were investigated for the transformed data. Another approach involved two-piece, double-exponential functions (Heaps, 1982; Rachele and Kilmer, 1991; Kilmer and Rachele, 1992a) such as

$$\sigma_e = A \exp\left[B \exp(Cz) \right] , \tag{1}$$

where A, B, and C are constants with appropriate values for the case being approximated. The latter approach was one of the more promising, but was not acceptable for our purposes. This was especially true for simulated backscatter coefficient profiles where the structure was too extensive to allow successful fitting by this approach. Specifically, we were searching for a continuous function that would result in a good fit over a wide range of points, while being constrained to fit the end points precisely. In particular, we wanted a function that required a minimum number of fitting constants, and we did not want to fit the entire curve by cutting it into several subsegments. For these reasons, we did not consider fitting with splines to be a desirable option.

2. THE R/K OPTICAL PROFILE FUNCTION

The R/K optical profile function is a higher order exponential written as

$$y = y_1 \left(\frac{y_2}{y_1} \right)^{M(x)} , \tag{2}$$

where

$$M(x) = \left(\frac{x - x_1}{x_2 - x_1} \right)^{N(x)} . \tag{3}$$

In equations (2) and (3), x is the independent variable and y is the dependent variable. The constraint points (end points) are designated as (x_1, y_1) and (x_2, y_2). N(x), a function of x, is represented in general form as

$$N(x) = \exp\left\{ a_o + \sum_{i=1}^{n} a_i x^i \right\} \tag{4}$$

or, for curves that contain oscillations,

$$N(x) = A_o + 2 \sum_{n=1}^{N_A} A_n \cos\left[\frac{2\pi n(x - x_{F1})}{x_{F2} - x_{F1} + 1} \right] - 2 \sum_{n=1}^{N_B} B_n \sin\left[\frac{2\pi n(x - x_{F1})}{x_{F2} - x_{F1} + 1} \right] \tag{5}$$

in the range $x_{F1} \le x \le x_{F2}$. In equations (4) and (5), A_o, A_1 through A_{NA}, B_1 through B_{NB}, x_{F1}, x_{F2}, a_o, and a_1 through a_n are constants. In our work we have found that n = 3 is generally sufficient when using equation (4) to fit extinction coefficient profiles; whereas, when fitting backscatter profiles, as many as 31 ($= 1 + N_A + N_B$) constants are used in equation (5).

To implement the functional structure defined by equations (2) through (5), we first solve equations (2) and (3) for N(x) giving

$$N(x) = \frac{\ln\left(\dfrac{\ln y - \ln y_1}{\ln y_2 - \ln y_1}\right)}{\ln\left(\dfrac{x - x_1}{x_2 - x_1}\right)} \quad . \tag{6}$$

Using some sets of N(x) data calculated according to equation (6), ln N(x) versus x data were fitted with polynomials to determine values of the constants in equation (4). Some other sets of N(x) data calculated according to equation (6) were fitted using Fourier analysis, resulting in the fitting expression given by equation (5). For some cases, one must use a combination of polynomial and Fourier terms. The polynomial and Fourier constants were determined by using IMSL (International Mathematical and Statistical Library) routines. All of the points (x, y) selected for fitting must be such that $x_1 < x < x_2$. All points used for polynomial fitting of ln N(x) must have y values such that $y_1 < y < y_2$.

3. EXAMPLES AND RESULTS

Values of (x_i, y_i) simulated by three different physical/mathematical models were considered in this study. For the first example, values (y_i) of extinction and backscatter coefficients simulated with the R/K microphysics model were considered. A plot of each of these simulated profiles is shown as solid lines in figures 1 and 2, where $z\,(=x)$ is the height above ground. For simulating data used in figure 1, model input included reference height (2 m above ground level) values of 95 percent, 5 km, and 0 °C for relative humidity, visibility, and ambient air temperature, respectively. Near adiabatic conditions and a maritime air mass were also selected. Model input for simulating data used in figure 2 also specified a maritime air mass, but a maximum liquid water content that would be 75 percent of the near adiabatic value was selected, and reference height values of 99 percent, 2 km, and 30 °C were specified for relative humidity, visibility, and ambient air temperature, respectively. These curves were considered as two segments for each case. The first segment represents the subcloud region for 2 m $\leq z \leq$ 103 m for extinction and 2 m $\leq z \leq$ 36 m for backscatter. The second segment represents the cloud region for 104 m $\leq z \leq$ 463 m and 37 m $\leq z \leq$ 460 m for extinction and backscatter, respectively. The fitting curves produced by equation (2) for extinction and backscatter coefficients are shown as dashed lines in figures 1 and 2. We considered the fits in each case to be very good. Values of R^2 (the coefficient of determination) were 0.99986 and 0.99855 for the fits shown in figures 1 and 2, respectively. The ln N(z) for extinction was fit with a cubic polynomial, figure 3. The fitting curve for backscatter shown in figure 4 was calculated by fitting ln N(z) with a cubic polynomial for the first segment and fitting N(z) with a 16-term Fourier series for the second segment. Note that even though the N(z) curves in figures 3, 4, and 6 are discontinuous at the cloud base, the corresponding σ_e and β curves are continuous as shown in figures 1, 2, and 5. As expected, the σ_e and β curves pass precisely through the specified values at the reference height (2 m), the cloud base, and the cloud top. Overall, the function fits of σ_e and β are very good. We did find, however, that for some cases a large number of Fourier terms were required to obtain a good fit. As an example, 31 Fourier terms were used for the second segment shown in figures 5 and 6.

For the second example, we used data produced by our* thermal conductivity model for loam soil, where k_s (= y) is the thermal conductivity and ϕ_w (= x) is the volume fraction of water. When generating the solid line curve shown in figure 7, we assumed that the volume fraction of solid material (sand, silt, and clay) was 0.5 and the volume fraction of organic matter was 0.10. This curve was fit by equation (2) for $0.2 \leq k_s \leq 2.1$ and $0 \leq \phi_w \leq 0.27$. Casual inspection shows that the fit is excellent. The ln $N(\phi_w)$ for this case was fit by a fourth degree polynomial, figure 8.

The third example makes use of a curve produced by our atmospheric planetary boundary layer model.** The solid line in figure 9 shows the change of wind direction α (= y) as a function of height z (= x), where α varies from 13° to 40° for $2 \text{ m} \leq z \leq 1000 \text{ m}$. The R/K fit to this curve is shown in figure 9. Again the fit is excellent. The ln N(z) values for this case were fit by a fourth degree polynomial, figure 10.

4. CONCLUSIONS

For the examples considered in this study, we found that the R/K optical profile function fits smooth model simulated curves very well. In a separate study (Kilmer and Rachele, 1992b), we fitted several hundred extinction and backscatter coefficient profiles with the R/K optical profile function and reached the same conclusion. Some cases, however, did require more terms than we would have liked when fitting N(z), σ_e, and β. Some backscatter coefficient curves with many large amplitude oscillations are examples of such cases. Some cases required both polynomial and Fourier terms.

* Rachele and Manguso, U.S. Army Research Laboratory, White Sands Missile Range, New Mexico, 88002. (Unpublished)

** Rachele, Hansen and Manguso, U.S. Army Research Laboratory, White Sands Missile Range, New Mexico 88002.

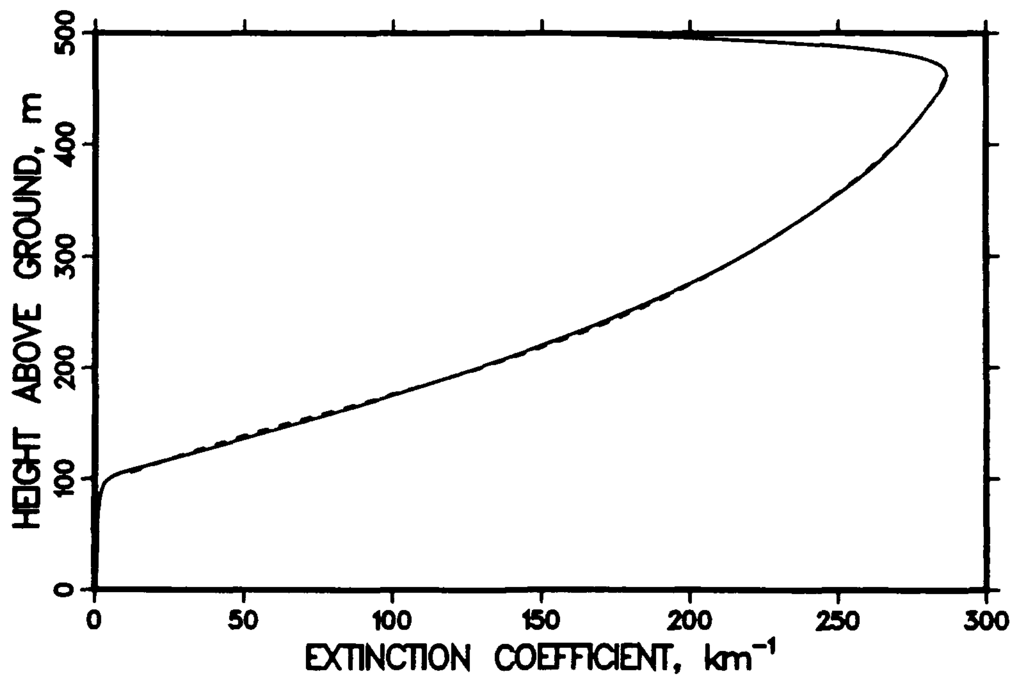

Figure 1. Solid line: R/K microphysics model simulation for a wavelength of 4.0 μm; dashes: calculated using R/K optical profile function as defined by equations (2), (3), and (4), with x = height, y = extinction coefficient, and n = 3.

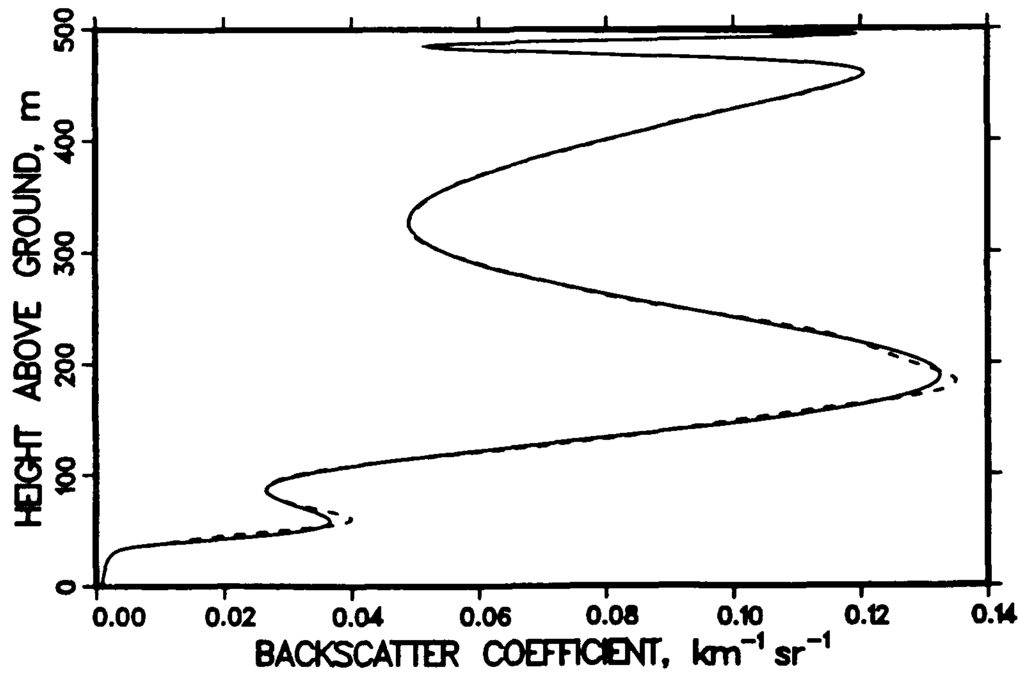

Figure 2. Solid line: R/K microphysics model simulation for a wavelength of 10.6 μm; dashes: calculated using R/K optical profile function as defined by equations (2), (3), and (4) (for $x \leq 36$ m) or (5) (for $x \geq 37$ m), with x = height, y = backscatter coefficient in equation (2), $N_A = 8$, and $N_B = 7$.

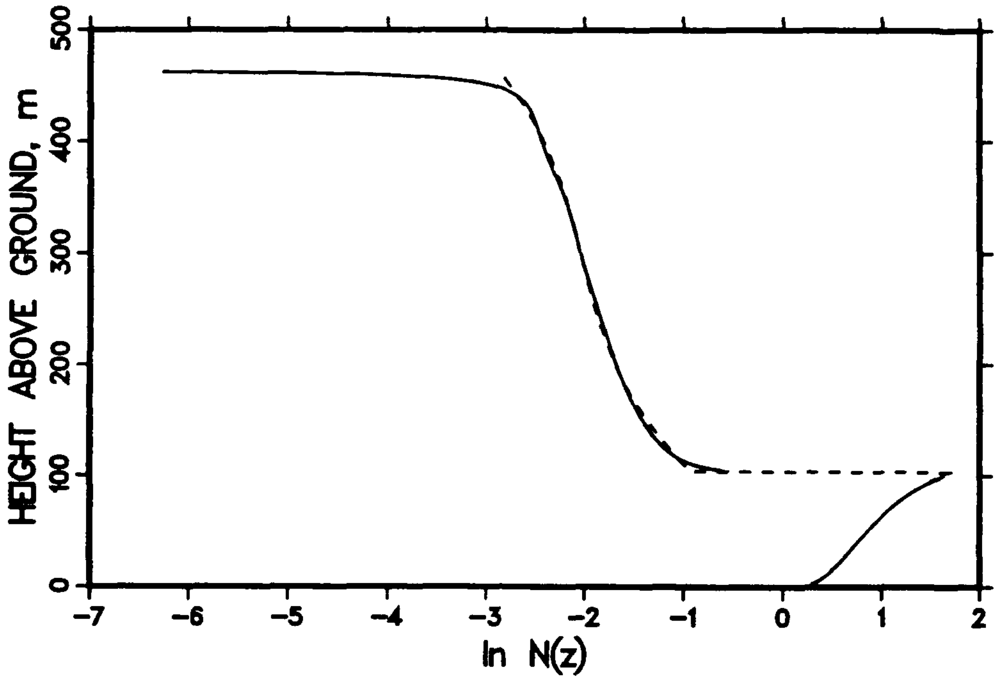

Figure 3. Solid line: R/K microphysics model simulation for a wavelength of 4.0 μm; dashes: calculated using equation (4), with x = height, y = extinction coefficient in equation (2), and n = 3.

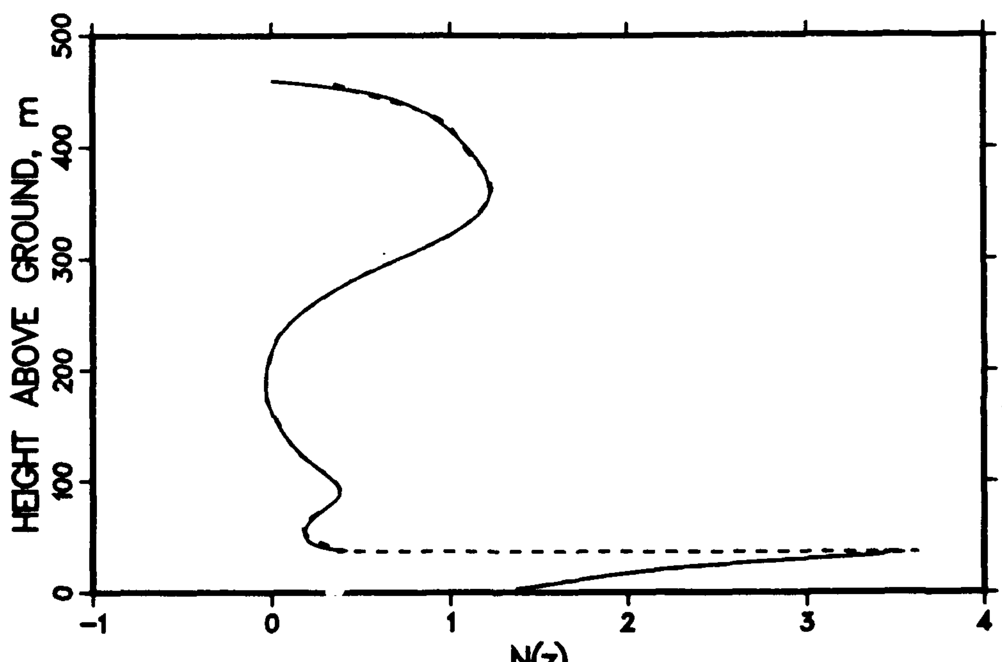

Figure 4. Solid line: R/K microphysics model simulation for a wavelength of 10.6 μm; dashes: calculated using equation (4) for $x \leq 36$ m and equation (5) for $x \geq 37$ m, with x = height, y = backscatter coefficient in equation (2), $N_A = 8$, and $N_B = 7$.

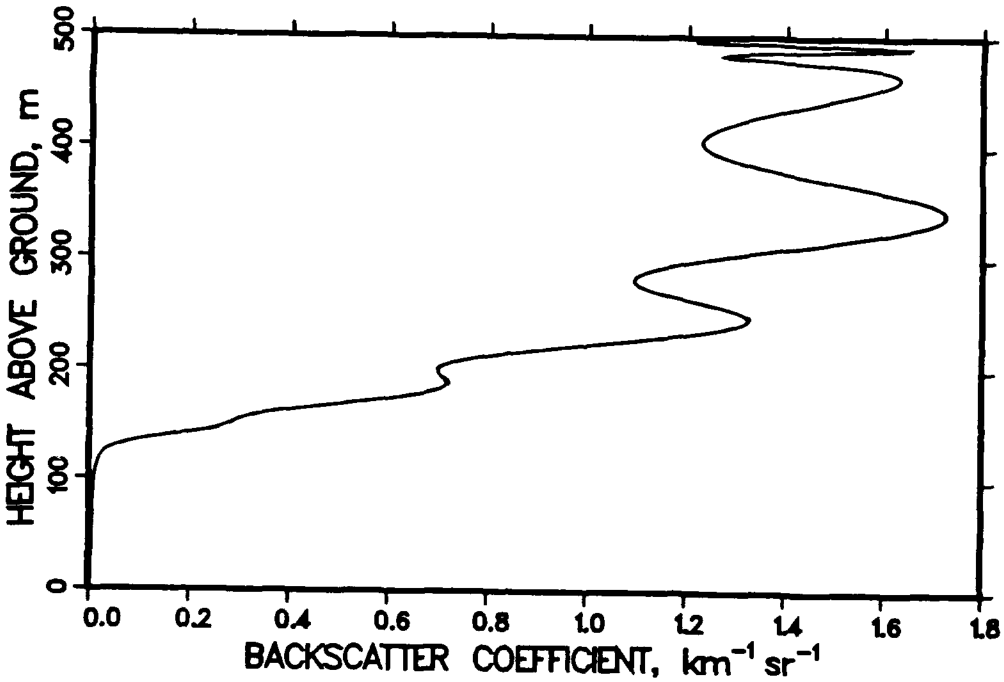

Figure 5. Solid line: 'K microphysics model simulation for a wavelength of 5.0 μm, maritime air mass, near adiabatic conditions, and reference height (2 m) values of 95 percent, 5 km, and 30 °C for relative humidity, visibility, and temperature, respectively. Dashes: calculated using R/K optical profile function as defined by equations (2), (3), and (4) (for $x \leq 129$ m) or (5) (for $x \geq 130$ m), with x = height, y = backscatter coefficient, and $N_A = N_B = 15$.

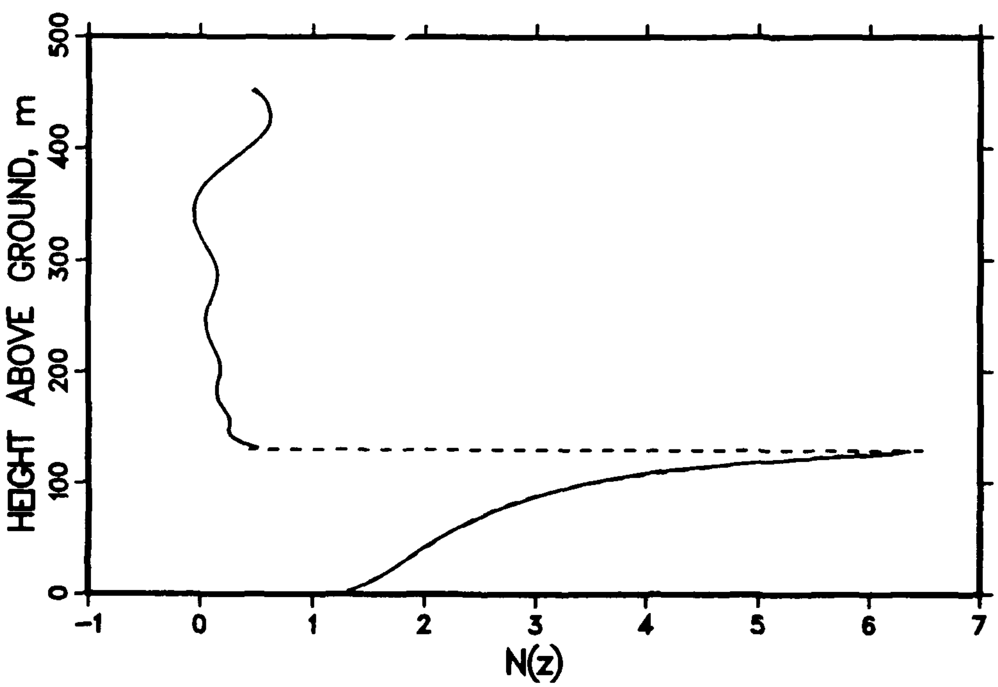

Figure 6. Solid line: R/K microphysics model simulation for same wavelength and case as in figure 5. Dashes: calculated using equation (4) for $x \leq 129$ m and equation (5) for $x \geq 130$ m, with x = height, y = backscatter coefficient in equation (2), and $N_A = N_B = 15$.

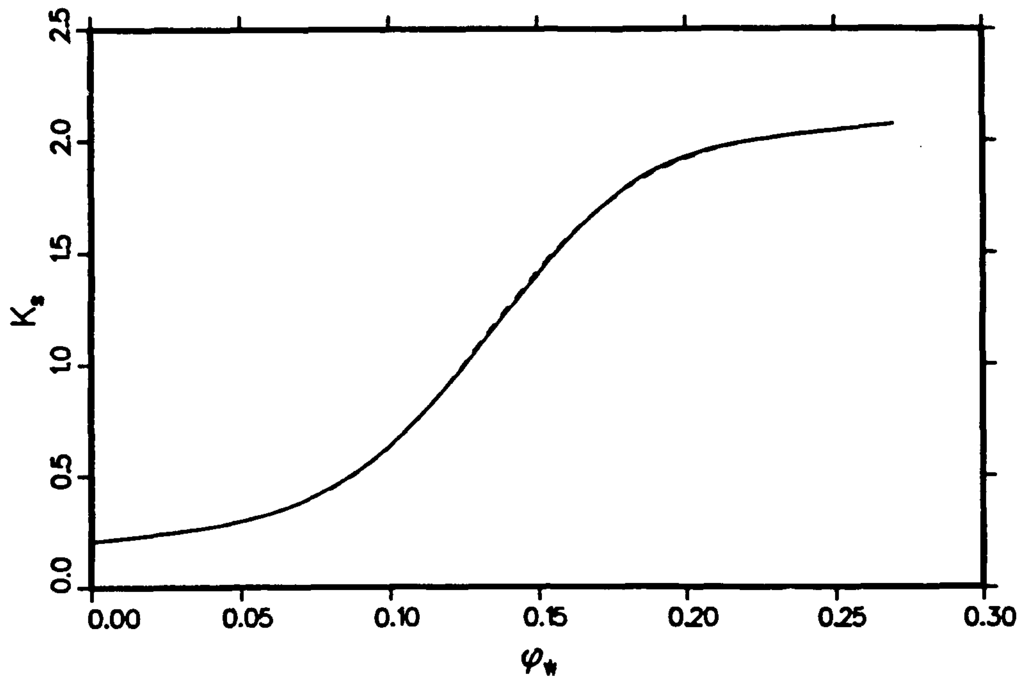

Figure 7. Thermal conductivity vs. water content for loam where $\phi_s = 0.5$, $\phi_q = 0.2$ \\\ fit with RK optical profile fit $N(\phi_w) = \exp(0.040407 + 3.3972\,\phi_w - 17.454\,\phi_w^2 - 769.18\,\phi_w^3 + 2460.47\,\phi_w^4$.

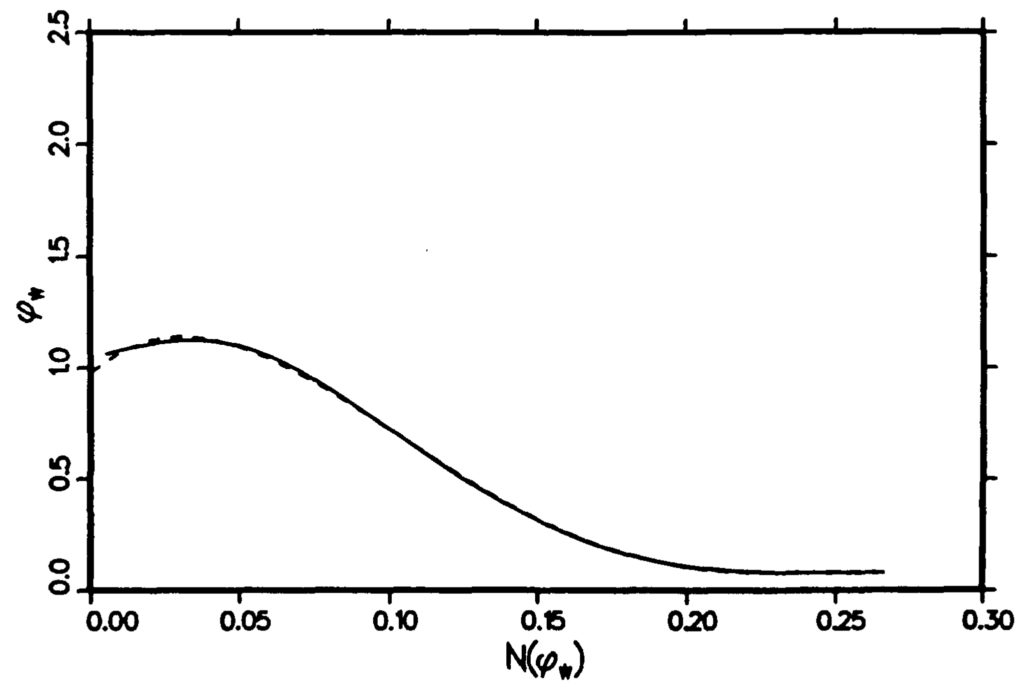

Figure 8. N(z) profile corresponding to figure 7.

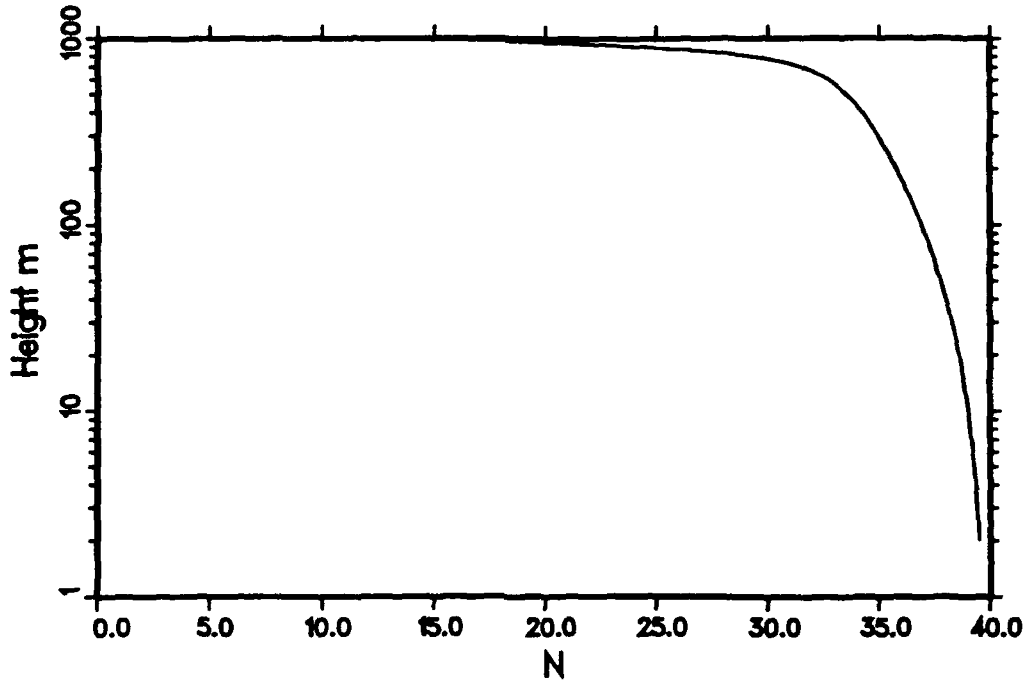

Figure 9. Wind turning angle, Nebraska data (8/19/53 16:35 CST) R/K optical profile fit with 4th degree polynomial fit for N. $\ln N(z) = -0.11031 + 3.08117 \times 10^{-3} z - 4.38265 \times 10^{-6} z^2 + 6.59899 \times 10^{-9} z^3 - 2.93911 \times 10^{-12} z^4$.

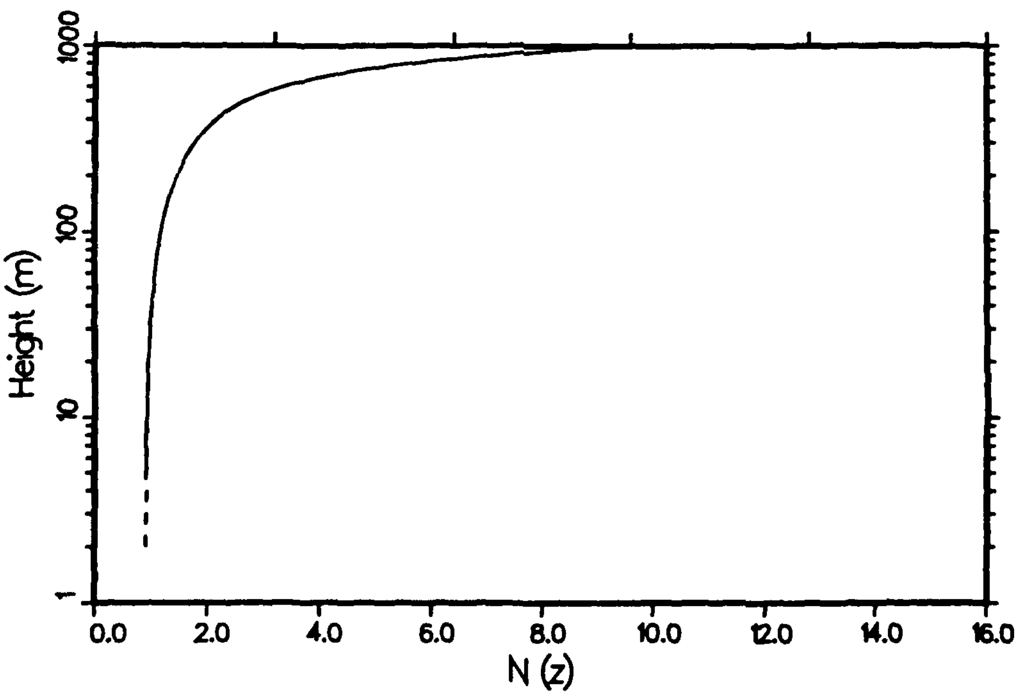

Figure 10. N(z) profile corresponding to figure 9.

REFERENCES

Duncan, L. D., J. D. Lindberg, and R. B. Loveland, 1980, An Empirical Model of the Vertical Structure of German Fogs, ASL-TR-0071, U.S. Army Atmospheric Sciences Laboratory, White Sands Missile Range, NM 88002.

Heaps, M. G., 1982, A Vertical Structure Algorithm for Low Visibility/Low Stratus Conditions, ASL-TR-0111, U.S. Army Atmospheric Sciences Laboratory, White Sands Missile Range, NM 88002.

Kilmer, N. H., and H. Rachele, 1992a, "Analytic Functions for Modeling Vertical Profiles of Extinction in and Beneath Very Low Stratus Clouds." In Atmospheric Propagation and Remote Sensing, Anton Kohnle and Walter B. Miller, eds., Proc. SPIE, 1688:132-143.

Kilmer, N. H., and H. Rachele, 1992b, "An Optical Profile Function for Modeling Extinction and Backscatter Coefficients in Very Low Stratus Clouds and Subcloud Regions." In Proceedings of the 1992 Battlefield Atmospherics Conference, U.S. Army Research Laboratory, White Sands Missile Range, NM 88002.

Rachele, H., and N. H. Kilmer, 1991, A Derivation for Determining Double Exponential Liquid Water Content and Extinction Profiles from Discrete Data, ASL-TR-0290, U.S. Army Atmospheric Sciences Laboratory, White Sands Missile Range, NM 88002.

Rachele, H., and N. H. Kilmer, 1992, Unified Very Low Stratus Cloud/Subcloud Microphysics Model, ASL Technical Report, ASL-TR-0309, U.S. Army Atmospheric Sciences Laboratory, White Sands Missile Range, NM 88002.

DISTRIBUTION LIST FOR PUBLIC RELEASE

Commandant
U.S. Army Chemical School
ATTN: ATZN-CM-CC (S. Barnes)
Fort McClellan, AL 36205-5020

Commander
U.S. Army Aviation Center
ATTN: ATZQ-D-MA
Mr. Oliver N. Heath
Fort Rucker, AL 36362

NASA/Marshall Space Flight Center
Deputy Director
Space Science Laboratory
Atmospheric Sciences Division
ATTN: E501 (Dr. George H. Fichtl)
Huntsville, AL 35802

NASA/Marshall Space Flight Center
Atmospheric Sciences Division
ATTN: Code ED-41
Huntsville, AL 35812

Deputy Commander
U.S. Army Strategic Defense Command
ATTN: CSSD-SL-L
Dr. Julius Q. Lilly
P.O. Box 1500
Huntsville, AL 35807-3801

Commander
U.S. Army Missile Command
ATTN: AMSMI-RD-AC-AD
Donald R. Peterson
Redstone Arsenal, AL 35898-5242

Commander
U.S. Army Missile Command
ATTN: AMSMI-RD-AS-SS
Huey F. Anderson
Redstone Arsenal, AL 35898-5253

Commander
U.S. Army Missile Command
ATTN: AMSMI-RD-AS-SS
B. Williams
Redstone Arsenal, AL 35898-5253

Commander
U.S. Army Missile Command
ATTN: AMSMI-RD-DE-SE
Gordon Lill, Jr.
Redstone Arsenal, AL 35898-5245

Commander
U.S. Army Missile Command
Redstone Scientific Information Center
ATTN: AMSMI-RD-CS-R/Documents
Redstone, Arsenal, AL 35898-5241

Commander
U.S. Army Intelligence Center and Fort Huachuca
ATTN: ATSI-CDC-C (Mr. Colanto)
Fort Huachuca, AZ 85613-7000

Northrup Corporation
Electronics Systems Division
ATTN: Dr. Richard D. Tooley
2301 West 120th Street, Box 5032
Hawthorne, CA 90251-5032

Commander - Code 3331
Naval Weapons Center
ATTN: Dr. Alexis Shlanta
China Lake, CA 93555

Commander
Pacific Missile Test Center
Geophysics Division
ATTN: Code 3250 (Terry E. Battalino)
Point Mugu, CA 93042-5000

Lockheed Missiles & Space Co., Inc.
Kenneth R. Hardy
Org/91-01 B/255
3251 Hanover Street
Palo Alto, CA 94304-1191

Commander
Naval Ocean Systems Center
ATTN: Code 54 (Dr. Juergen Richter)
San Diego, CA 92152-5000

Meteorologist in Charge
Kwajalein Missile Range
P.O. Box 67
APO San Francisco, CA 96555

U.S. Department of Commerce
Mountain Administration Support
Center
Library, R-51 Technical Reports
325 S. Broadway
Boulder, CO 80303

Dr. Hans J. Liebe
NTIA/ITS S 3
325 S. Broadway
Boulder, CO 80303

NCAR Library Serials
National Center for Atmos Rsch
P.O. Box 3000
Boulder, CO 80307-3000

HQDA
ATTN: DAMI-POI
Washington, DC 20310-1067

Mil Asst for Env Sci Ofc of
The Undersecretary of Defense
for Rsch & Engr/R&AT/E&LS
Pentagon - Room 3D129
Washington, DC 20301-3080

Director
Naval Research Laboratory
ATTN: Code 4110
Dr. Lothar H. Ruhnke
Washington, DC 20375-5000

HQDA
DEAN-RMD/Dr. Gomez
Washington, DC 20314

Director
Division of Atmospheric Science
National Science Foundation
ATTN: Dr. Eugene W. Bierly
1800 G. Street, N.W.
Washington, DC 20550

Commander
Space & Naval Warfare System Command
ATTN: PMW-145-1G (LT Painter)
Washington, DC 20362-5100

Commandant
U.S. Army Infantry
ATTN: ATSH-CD-CS-OR
Dr. E. Dutoit
Fort Benning, GA 30905-5090

USAFETAC/DNE
Scott AFB, IL 62225

Air Weather Service
Technical Library - FL4414
Scott AFB, IL 62225-5458

HQ AWS/DOO
Scott AFB, IL 62225-5008

USAFETAC/DNE
ATTN: Mr. Charles Glauber
Scott AFB, IL 62225-5008

Commander
U.S. Army Combined Arms Combat
ATTN: ATZL-CAW (LTC A. Kyle)
Fort Leavenworth, KS 66027-5300

Commander
U.S. Army Space Institute
ATTN: ATZI-SI (Maj Koepsell)
Fort Leavenworth, KS 66027-5300

Commander
U.S. Army Space Institute
ATTN: ATZL-SI-D
Fort Leavenworth, KS 66027-7300

Commander
Phillips Lab
ATTN: PL/LYP (Mr. Chisholm)
Hanscom AFB, MA 01731-5000

Director
Atmospheric Sciences Division
Geophysics Directorate
Phillips Lab
ATTN: Dr. Robert A. McClatchey
Hanscom AFB, MA 01731-5000

Raytheon Company
Dr. Charles M. Sonnenschein
Equipment Division
528 Boston Post Road
Sudbury, MA 01776
Mail Stop 1K9

Director
U.S. Army Materiel Systems
Analysis Activity
ATTN: AMXSY-MP (H. Cohen)
APG, MD 21005-5071

Commander
U.S. Army Chemical Rsch,
Dev & Engr Center
ATTN: SMCCR-OPA (Ronald Pennsyle)
APG, MD 21010-5423

Commander
U.S. Army Chemical Rsch,
Dev & Engr Center
ATTN: SMCCR-RS (Mr. Joseph Vervier)
APG, MD 21010-5423

Commander
U.S. Army Chemical Rsch,
Dev & Engr Center
ATTN: SMCCR-MUC (Mr. A. Van De Wal)
APG, MD 21010-5423

Director
U.S. Army Materiel Systems
Analysis Activity
ATTN: AMXSY-AT (Mr. Fred Campbell)
APG, MD 21005-5071

Director
U.S. Army Materiel Systems
Analysis Activity
ATTN: AMXSY-CR (Robert N. Marchetti)
APG, MD 21005-5071

Director
U.S. Army Materiel Systems
Analysis Activity
ATTN: AMXSY-CS (Mr. Brad W. Bradley)
APG, MD 21005-5071

Commander
U.S. Army Laboratory Command
ATTN: AMSLC-CG
2800 Powder Mill Road
Adelphi, MD 20783-1145

Commander
Headquarters
U.S. Army Laboratory Command
ATTN: AMSLC-CT
2800 Powder Mill Road
Adelphi, MD 20783-1145

Commander
Harry Diamond Laboratories
ATTN: SLCIS-CO
2800 Powder Mill Road
Adelphi, MD 20783-1197

Director
Harry Diamond Laboratories
ATTN: SLCHD-ST-SP
Dr. Z.G. Sztankay
Adelphi, MD 20783-1197

National Security Agency
ATTN: W21 (Dr. Longbothum)
9800 Savage Road
Ft George G. Meade, MD 20755-6000

U. S. Army Space Technology
and Research Office
ATTN: Brenda Brathwaite
5321 Riggs Road
Gaithersburg, MD 20882

OIC-NAVSWC
Technical Library (Code E-232)
Silver Springs, MD 20903-5000

The Environmental Research
Institute of MI
ATTN: IRIA Library
P.O. Box 134001
Ann Arbor, MI 48113-4001

Commander
U.S. Army Research Office
ATTN: DRXRO-GS (Dr. W.A. Flood)
P.O. Box 12211
Research Triangle Park, NC 27709

Dr. Jerry Davis
North Carolina State University
Department of Marine, Earth, &
Atmospheric Sciences
P.O. Box 8208
Raleigh, NC 27650-8208

Commander
U. S. Army CECRL
ATTN: CECRL-RG (Dr. H. S. Boyne)
Hanover, NH 03755-1290

Commanding Officer
U.S. Army ARDEC
ATTN: SMCAR-IMI-I, Bldg 59
Dover, NJ 07806-5000

U.S. Army Communications-Electronics
Command EW/RSTA Directorate
ATTN: AMSEL-RD-EW-OP
Fort Monmouth, NJ 07703-5206

Commander
U.S. Army Satellite Comm Agency
ATTN: DRCPM-SC-3
Fort Monmouth, NJ 07703-5303

6585th TG (AFSC)
ATTN: RX (CPT Stein)
Holloman AFB, NM 88330

Department of the Air Force
OL/A 2nd Weather Squadron (MAC)
Holloman AFB, NM 88330-5000

PL/WE
Kirtland AFB, NM 87118-6008

Director
U.S. Army TRADOC Analysis Command
ATTN: ATRC-WSS-R
White Sands Missile Range, NM 88002

Rome Laboratory
ATTN: Technical Library RL/DOVL
Griffiss AFB, NY 13441-5700

Department of the Air Force
7th Squadron
APO, NY 09403

AWS
USAREUR/AEAWX
APO, NY 09403-5000

AFMC/DOW
Wright-Patterson AFB, OH 0334-5000

Commandant
U.S. Army Field Artillery School
ATTN: ATSF-TSM-TA
Mr. Charles Taylor
Fort Sill, OK 73503-5600

Commander
Naval Air Development Center
ATTN: Al Salik (Code 5012)
Warminister, PA 18974

Commander
U.S. Army Dugway Proving Ground
ATTN: STEDP-MT-DA-M
Mr. Paul Carlson
Dugway, UT 84022

Commander
U.S. Army Dugway Proving Ground
ATTN: STEDP-MT-DA-L
Dugway, UT 84022

Commander
U.S. Army Dugway Proving Ground
ATTN: STEDP-MT-M (Mr. Bowers)
Dugway, UT 84022-5000

Defense Technical Information Center
ATTN: DTIC-FDAC
Cameron Station
Alexandria, VA 22314

Commanding Officer
U.S. Army Foreign Science &
Technology Center
ATTN: CM
220 7th Street, NE
Charlottesville, VA 22901-5396

Naval Surface Weapons Center
Code G63
Dahlgren, VA 22448-5000

Commander
U.S. Army OEC
ATTN: CSTE-EFS
Park Center IV
4501 Ford Ave
Alexandria, VA 22302-1458

Commander and Director
U.S. Army Corps of Engineers
Engineer Topographics Laboratory
ATTN: ETL-GS-LB
Fort Belvoir, VA 22060

TAC/DOWP
Langley AFB, VA 23665-5524

U.S. Army Topo Engineering Center
ATTN: CETEC-ZC
Fort Belvoir, VA 22060-5546

Commander
Logistics Center
ATTN: ATCL-CE
Fort Lee, VA 23801-6000

Commander
USATRADOC
ATTN: ATCD-FA
Fort Monroe, VA 23651-5170

Science and Technology
101 Research Drive
Hampton, VA 23666-1340

Commander
U.S. Army Nuclear & Cml Agency
ATTN: MONA-ZB Bldg 2073
Springfield, VA 22150-3198